ISSN 0965-545X, Polymer Science, Series A, 2021, Vol. 63, Suppl. 1, pp. S46–S57. © Pleiades Publishing, Ltd., 2021.
ISSN 0965-545X, Polymer Science, Series A, 2022. © Pleiades Publishing, Ltd., 2022.

POLYMER BLENDS

Effect of Compatibilization of Thermoplastic Polyurethane with Poly(lactic acid) for the Preparation of Sustainable Blends

K. A. Rajesh[a],*, Arun. M. Panicker[a], and T. O. Varghese[a]

[a]*Central Institute of Plastics Engineering and Technology (CIPET), Eloor, Udyogamandal P.O., Kochi, Kerala, 683501 India*

**e-mail: rajeshcipet@gmail.com*

Received December 25, 2021; revised January 18, 2022; accepted January 21, 2022

Abstract—Poly(lactic acid) (PLA) is a prominent biopolymer highly recommended for resolving environmental concerns due to its biodegradability. To overcome its limitations of brittleness, blending with other polymers is common technique but results in phase separation. In this work, impact modification of poly(lactic acid) (PLA) has been carried out by melt blending with maleic anhydride grafted thermoplastic polyurethane (PLMTPU) and with acrylonitrile grafted thermoplastic polyurethane (PLATPU). The blends were prepared using twin screw extruder by melt mixing of PLA with grafted TPUs in ratios of 97.5/2.5, 95/5, 92.5/7.5, and 90/10 by weight percentage. The interfacial adhesion imparted through compatibilization shown pronounced improvement in the impact strength of PLATPU and PLMTPU by 88 and 28% respectively compared to the virgin PLA. Also, improvement in the elongation at break from 1.2% (PLA) to 4.4% (PLATPU) and 4.9% (PLMTPU) was observed. The mechanical studies were also compared with the theoretical models. Interestingly, incorporated flexibility to the PLA with ATPU and MTPU and the impeded effective stress transfer mechanism was evident on probing the morphology of the blends. The novel compatibilized blend of PLA with grafted TPU is potential candidate for packaging, biomedical applications and as a feed stock material in 3D printing technologies.

DOI: 10.1134/S0965545X22030087

INTRODUCTION

In recent times, quite an interest is flourishing in the development of bio-based polymer systems in disparate level of applications like structural, biomedical, pharmaceutical etc. The short in the resources, insecure pricing level, contribution in climate change, and problem related to waste disposal fueled the development of polymers from renewable resources than the polymers from the fossil fuel. Industrialization of biopolymers is still evolving and expected to be in a remarkable level in the coming years.

Poly(lactic acid) (PLA) is an important biopolymer, ubiquitous in every field of research owing to its peculiar features like biodegradability, high stiffness, strength, high workability and transparency etc. [1]. In order to overcome the impairments of unmodified PLA like brittleness, low impact strength and elongation at break, blending can be adopted [2]. Enhancement in the toughness and stress elongation of PLA has been observed in the studies, where, addition of rigid fillers, blending with polymers, flexible fillers or elastomers, co-polymerization, and plasticization has been executed. As reported, coir fibre [3], sugarcane bagasse fibre [4], flax fibre [5], sisal and hemp fibre, cotton fibre [6], banana/sisal fibre [7], Surface treated cellulose fibre reinforced PLA composite materials exhibits an improved elongation at break [8]. Various blends of PLA has been studied with elastomeric polymers such as low density polyethylene [9], polypropylene [10], polyethylene glycol [11], and natural rubber [12] and which are showed a plasticizing effect on PLA. Fully compatible low molecular weight substances, as well as miscible or immiscible polymer blends of PLA with flexible polymers, results in the molecules of the heterogenous phase to act as flexibile moieties within the molecular framework of PLA and hence effectively lowering glass transition temperature T_g and in turn resulting in improved impact properties. PLA blending offers a cost-effective option in comparison to other impact modification methodologies. Copolymerization is also employed in tailoring the tensile and impact properties of PLA to desired outcomes through polycondensation of lactic acid (LA) with other monomers (or oligomers) or ring-opening copolymerization (ROC) of LA with other cyclic monomers (or oligomers), wherein ROC synthesis method is extensively employed for the high molecular weight copolymers. Consequently, plasticization of PLA with plasticizers/modifiers, viz. oligomeric malonate ester amides [13], bifunctional cyclic esters [14], citrate esters [15], 4,4'-methylene diphenyl diisocyanate [16], polymerized soybean oil [17], polyethylene glycol and acetyl triethyl citrate etc. [18] have been found to impart good processability, flexibility

and ductility to the glassy PLA matrix. However, the high cost of copolymerization and the migration of low molecular weight plasticizers from PLA matrix during modification by plasticization make these processes unsuitable for wider implementation. From these approaches blending can be said to be the most effective and the simplest process.

In polymer blending a new material having different physical properties is created from at least two polymers. In which compatible polymer blends are immiscible blends with macroscopically uniform physical properties and it is achieved from the strong interactions among the component polymers. Twin screw extruders are often used for the blending of polymers in an industrial scale. The physical blending of PLA is challenging due to its intrinsic immiscibility, inferior compatibility, and destitute interfacial bonding between the blend components [19].

In several studies toughening of PLA was investigated with flexible, biocompatible TPU elastomers. TPU is a block copolymer having alternate hard segments (diisocyanates) and soft segments (polyester or polyether based polyol) [20]. Owing to the fact that TPU bears lower glass transition temperature and high thermal stability, blending with PLA is more easier [21]. It has been reported that, the brittle nature of PLA became ductile after blending with TPU [22]. In several studies, elongation at break and impact strength were found to enhance during blending with TPU [23, 24].

However, the compatibility between TPU and PLA is poor and needs to improve for achieving in-depth properties and extent the applicability of the blend. Kahraman et al., reported that PLA/TPU blend system with enhanced phase compatibility, impact strength and ductility with the advent of multifunctional epoxy Joncryl ADR 4468 chain extender (CE) [25]. In one of the studies by Kilic et al., PLA/TPU has been compatibilized using triglycidylisobutyl polyhedral oligomeric silsesquioxane and reported a considerable decrease in the tensile strength and increase in the impact strength over blending process [26]. In another study a ternary blend system of, thermoplastic polyurethane/poly (*D*-lactic) acid/poly (*L*-lactic) acid (TPU/PDLA/PLLA) was reported with the maximum value of tensile strength, elongation at break, and fracture work of ternary blends are 61.9 MPa, 23.5%, and 1038.9 kJ/m^3, respectively [27]. However, the use of chain extenders inversely affects the biodegradability owing to the increased hard segment content [28]. Majority of the blend system of PLA with TPU reported in the literature are of higher blend ratio by reducing more PLA content.

Previously reported studies were done with higher percentages of TPU content in the PLA blend and these effected in poor miscibility, processability, and biodegradability. In this work, we focused on an overall magnification of the properties of PLA without compromising the biodegradability of PLA. The study was successfully imparted impact modification on PLA with maleic anhydride grafted thermoplastic polyurethane (PLMTPU) and with acrylonitrile grafted thermoplastic polyurethane (PLATPU). The melt blending processes were carried out in a twin screw extruder with PLA and grafted TPUs in ratios of 97.5/2.5, 95/5, 92.5/7.5, and 90/10 by weight percentage. The interfacial compatibility and strong bonding among the blend components resulted in blends with desirable properties. The resulted novel PLA blends ensures minimal carbon foot print and promises the extent of applicability of PLA.

EXPERIMENTAL

Materials

Poly(lactic acid) injection moulding grade, Ingeo 3052D (M.W: 116000 g/mol, Specific gravity: 1.24 g/cm^3, and MFI (210°C and 2.16 kg load): 14 g/10 min) was procured from Nature Works LLC, USA. Thermoplastic polyurethane (TPU) used in this work is Desmopan 385 E Ester type injection moulding grade was bought from Bayer Material science AG, USA. Acrylonitrile (AN) monomer with purity ≥99%, Sodium hydroxide (≥97%), and dicumyl peroxide (≥97.5%) were purchased from Zigma Aldrich. Maleic anhydride with ≥ 99% was obtained from Loba Chemie. Acetone with ≥99% (M.W: 58.08 g/mol) procured from Merck. All allied chemicals used in this study were analytical grade.

Sample Preparation

Grafting. Preparation of ATPU and MTPU were carried out in a co-rotating twin-screw extruder (model-ZV20, Specific Engineering). Dicumyl peroxide (DCP) was used as the free radical initiator. For the preparation of ATPU, Acrylonitrile monomer was washed with 3% NaOH and 3% Orthophosphoric acid to render inhibitor free for three times and checked for neutral pH. Further acrylonitrile (AN) monomer was washed with distilled water and dried using molecular sieves 4 Å × 1.5 mm. 20 g dried DC reprecipitated from methanol (2% of total weight) was mixed well with 900 g TPU. 100 mL AN was taken in a flow rate estimated burette. TPU was added through the hopper while AN was added directly into the extruder barrel using a burette. The screw speed was set at 60 rpm and the temperature profile was maintained at 165, 175, 185, 195, 200, and 205°C at melt pressure of 5–15 bar. The resulting AN grafted TPU (ATPU) was pelletized, washed repeatedly with demineralized water and dried in hot air oven overnight at 100 ± 5°C to constant weight.

Table 1. Compositions of PLATPU and PLMTPU blends and melting and crystallization parameters of PLA, PLATPU, and PLMTPU

PLA, wt %	TPU, wt %	Volume fraction Φ_d	Sample code	T_g, °C	T_{cc}, °C	ΔH_{cc}, J/g	T_m, °C	ΔH_m, J/g	X_c, %
100	0	0	PLA	61	115	34	150	37	40
97.5	2.5	0.03	2.5PLATPU	64	134	10	149	11	12
95.0	5.0	0.05	5PLATPU	64	132	13	148	15	17
92.5	7.5	0.08	7.5PLATPU	64	133	14	148	16	18
90.0	10.0	0.10	10PLATPU	64	133	13	148	15	18
97.5	2.5	0.03	2.5PLMTPU	62	131	18	147	20	22
95.0	5.0	0.05	5PLMTPU	61	130	25	147	23	10
92.5	7.5	0.08	7.5PLMTPU	59	129	23	146	24	28
90.0	10.0	0.10	10PLMTPU	58	123	27	144	30	4

Further grafting of MA on TPU was carried using the same technique. In this case DCP was reprecipitated from acetone. Then, MA was mixed with TPU and fed into the extruder hopper at 0.3 and 10% compositions respectively. The extruder was set in a temperature profile of 165–205°C and at pressure of 10–15 bar. The extruded MA grafted TPU (MTPU) was pelletized, washed, and drying was carried out at 100 ± 5°C overnight in a hot air oven and stored in airtight polybags.

In both cases percentage yield of graft was estimated by the Eq. (1) [29]:

$$\%\ \text{Graft yield} = \frac{\text{Dry weight of grafted TPU} - \text{Dry weight of TPU}}{\text{Dry weight of TPU}} \times 100. \quad (1)$$

Preparation of blends. Binary blends of PLA with Acrylonitrile grafted Thermoplastic Polyurethane (ATPU) and Maleic Anhydride grafted Thermoplastic Polyurethane (MTPU) were prepared by melt blending process using co-rotating twin-screw extruder (model-ZV20). Resulting blends were characterized in correlation to their dispersed phase volume fractions Φ_d and calculated according to the Eq. (2):

$$\Phi_d = \frac{\left(\frac{W_d}{\rho_d}\right)}{\left[\left(\frac{W_d}{\rho_d}\right) + \left(\frac{W_c}{\rho_c}\right)\right]}, \quad (2)$$

where W is the weight fractions and ρ is the density of the constituents wherein subscripts *d* and *c* denote dispersed phase and continuous phases respectively. Table 1 enlists the details of blend formulations and their corresponding Φ_d values.

Preparation of test specimens. Test specimens were prepared by injection moulding technique using automatic injection moulding machine (Model-OMEGA 80 WIDE, Ferromatik Milacron). A temperature profile of 180 to 200°C was maintained while the injection pressure and mould temperature was 60 bar and 30°C respectively.

Experimental Techniques

Fourier transform infrared spectroscopy. Grafting of AN and MA were confirmed by FTIR and the study was conducted with Avatar 370 FTIR, Thermo Nicolet (Thermofisher Scientific, MA, USA) spectrophotometer. Scanning were done on dried powdered samples over a range of 400–4000 cm^{-1} at a resolution of 4 cm^{-1}.

Thermal characterizations. Thermal characteristics of prepared blends were obtained by means of DSC at a heating range of 20 to 200°C and 20 K/min heating rate using TA Instruments-Q20 (New Castle, DE) differential scanning calorimeter. Specimens for the test were prepared by injection moulding technique. The thermal stability of the blends was analyzed by TGA using TGA-Q50 thermogravimetric analyzer (TA Instruments Inc., New Castle, USA). The test was carried out over a temperature range of 30 to 600°C at a scan rate of 10 K/min. For this 5–10 mg of sample was taken from the injection moulded specimen.

Mechanical study. Tensile and flexural tests were performed on universal testing machine (UTM) Tinius Olsen H50KL (Tinius Olsen) at 23 ± 2°C and 50 ± 5% RH by following ASTM D 638 and ASTM D 790 respectively. For the tensile test, cross-head speed of 50 mm/min was used. Flexural tests were conducted at a cross-head bending speed of 2.5 mm/min and span distance of 96 mm. Notched Izod impact strength was

Table 2. Mechanical properties of PLA, PLATPU, and PLMTPU blends

Sample code	Tensile modulus, MPa	Increase of tensile modulus, %	Tensile strength, MPa	Increase of tensile strength, %	Elongation at break, %	Increase of elongation at break, %	Impact strength, kJ/m^2	Increase of impact strength, %
PLA	3280 ± 150	–	38.27 ± 7.00	–	1.20 ± 0.50	–	1.64 ± 0.50	–
2.5PLATPU	3040 ± 300	–7.22	45.10 ± 0.50	17.86	3.88 ± 1.00	224.14	2.07 ± 0.50	25.83
5PLATPU	3035 ± 20	–7.38	43.30 ± 1.00	13.15	4.38 ± 1.00	266.19	2.63 ± 0.50	60.14
7.5PLATPU	2980 ± 100	–9.05	39.73 ± 2.00	3.83	3.94 ± 1.00	228.88	3.10 ± 0.50	88.80
10PLATPU	2590 ± 100	–20.96	35.57 ± 6.00	–7.06	3.55 ± 1.00	196.85	2.80 ± 0.50	70.63
2.5PLMTPU	2977 ± 70	–9.16	51.77 ± 1	35.28	4.93 ± 1	311.86	1.68 ± 0.50	2.60
5PLMTPU	3085 ± 80	–5.85	43.00 ± 1	12.37	3.56 ± 1.22	197.41	1.81 ± 0.50	10.34
7.5PLMTPU	2860 ± 150	–12.72	42.23 ± 1	10.37	2.89 ± 0.94	141.72	2.10 ± 0.50	27.86
10PLMTPU	2920 ± 300	–10.78	38.67 ± 2	1.05	2.43 ± 0.83	103.01	1.71 ± 0.50	4.26

measured on Tinius Olsen Model Impact 104 machine following ASTM D 256 specifications. A minimum of five specimens were tested and reported the average values.

Morphological analysis. Evaluation of the morphology of the PLA blends was studied by SEM using JEOL Model, JSM-6390 L V under an accelerating voltage of 10 kV. Impact fractured specimens with gold sputtering were used for the test.

RESULTS AND DISCUSSION

Figure 1 shows the FTIR spectra of pure TPU, ATPU, and MTPU. On analyzing the FTIR spectra of TPU, ATPU, and MTPU, peaks present in the region of 3300–3340 cm^{-1} corresponds to the stretching vibration of OH groups. On analyzing TPU spectra NH stretching and deformation were present at 3338 and 1530 cm^{-1} respectively. We may observe symmetric and asymmetric CH vibrations at 2955 and 2922 cm^{-1} [30, 31]. In the case of TPU, NH bending peak can be observed at 1533 cm^{-1} [32]. The carbonyl index calculated for MTPU was 1.24. The peak at 1700 cm^{-1} reveals good degree of cyclic maleic anhydride grafting with the shift in peak of carbonyl group of TPU to higher energy wavelength. Grafting of AN over TPU was confirmed by the presence of C≡N stretching at 2232 cm^{-1}. The signs of maleation were evident from the spectra and these includes a small shoulder in the 1725 cm^{-1} can be due to C=O, peak at 1875 cm^{-1} corresponds to the COOH, and peaks present in the region from 1699 to 1076 cm^{-1} attributes to C=C in the MA [33, 34].

Table 3. Adhesion parameter k, Eq. (4), Stress concentration factor α, Eq. (5), and parameter representing load bearing capacity of disperse phase B, Eq. (6) in PLATPU and PLMTPU blends

Φ_d	PLATPU			PLMTPU		
	k	α	B	k	α	B
0.03	–2.04	–6.37	9.80	–4.04	–11.71	15.14
0.05	–0.95	–2.40	5.77	–0.89	–2.26	5.64
0.08	–0.21	–0.49	3.81	–0.57	–1.28	4.60
0.10	0.32	0.71	2.57	–0.05	–0.10	3.38
Mean value	–0.72	–2.13	5.49	–1.39	–3.84	7.19

DSC heating scans of the samples are depicted in the Fig. 2 and the corresponding parameters are enlisted in Table 1. The T_g value of PLA was observed at 61°C and it is in accordance with the literature [35]. On analyzing the thermal characteristics of blends there observed a slight increment in the T_g value on the addition of ATPU. This can be due to the dipole interaction between the –CN groups in the ATPU with the chains of PLA. Mobility of the polymer chain get restricted with the increase in the dipole interaction [36, 37]. While the MTPU addition caused decrement in the T_g value and it can be accredited to the increased compatibility between the polymers [38]. The decrease in the T_g value also has the significance in interface adhesion and it can be defined in terms of strong bonding among the polymers [39]. The compatibilization effect of ATPU and MTPU on blending with PLA is evident from the DSC scans which shows a single melting peak corresponding to PLA (at ca. 145°C).

The melting peaks in PLATPU and PLMTPU blends can be accredited to the crystallization of PLA. The percentage of crystallinity of PLATPU and PLMTPU decreased compared to PLA and it can be accredited to the soft segments present in the TPU. This is because of the decrease in the inter and intramolecular forces and caused flexibility to the

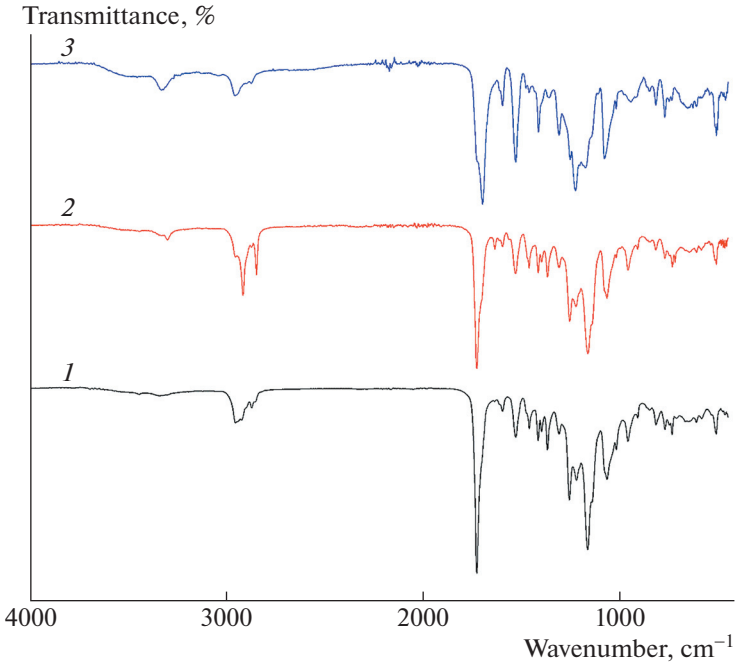

Fig. 1. FTIR spectra of (*1*) TPU, (*2*) ATPU, and (*3*) MTPU.

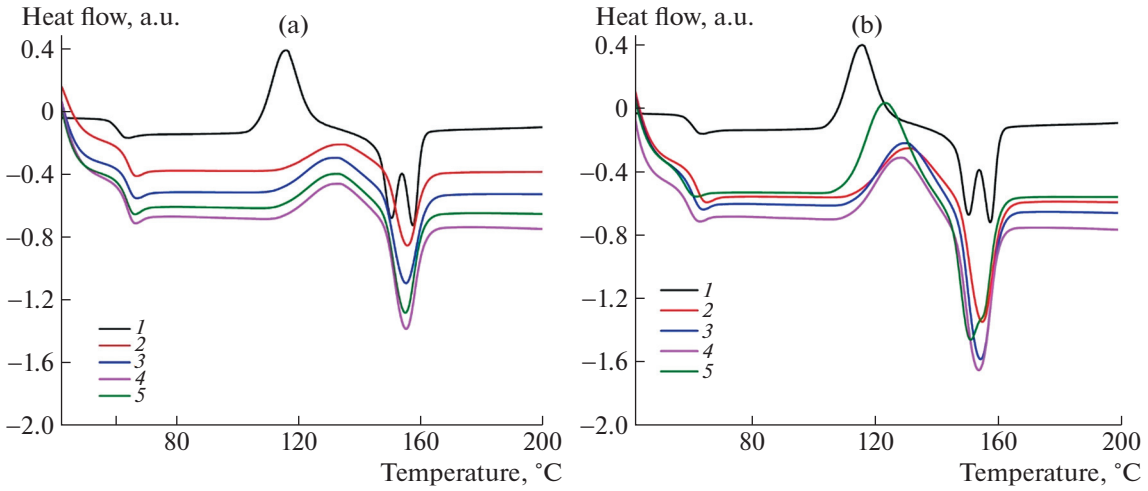

Fig. 2. DSC thermograms of (*1*) PLA, (a) (*2*) 2.5PLATPU, (*3*) 5PLATPU, (*4*) 7.5PLATPU, (*5*) 10PLATPU, (b) (*2*) 2.5PLMTPU, (*3*) 5PLMTPU, (*4*) 7.5PLMTPU, (*5*) 10PLMTPU.

PLA chains and this leads to the decrease in crystallinity [40].

The results of thermal stability studies of virgin PLA and PLATPU, PLMTPU blends are summarized in Table 4. Onset temperature of degradation of PLA was 316.8°C and the major degradation process was completed by 340.4°C (Fig. 3). It was noted that all the blend compositions had higher onset, maximum degradation temperature and peak degradation values compared to virgin PLA. The major degradation stage of PLA/TPU blends took place in the temperature range of 320 to 380°C. The increase in thermal stability of PLATPU and PLMTPU blends compared to PLA may be attributed to the blend component TPU absorbing more energy and consequent delay in the degradation onset of PLA [41]. The presence of MA and AN units also contributes to the thermal stability of the blend system [42].

Typically, PLA suffers from strain localization induced by strong strain softening and insufficient strain hardening at break, leading to tri-axial stress concentration [43]. Consequently, the local tri-axial

Table 4. Thermal properties of PLA, PLATPU and PLMTPU

Sample	Onset degradation temperature T_{onset}, °C	Peak degradation temperature T_{peak}, °C	Maximum degradation temperature T_{max}, °C	Maximum weight loss rate W, %/°C
PLA	316.8	336.9	340.4	–3.2
2.5PLATPU	332.1	369.1	376.0	–3.4
5PLATPU	336.8	365.2	372.9	–2.6
7.5PLATPU	333.8	363.8	375.9	–2.4
10PLATPU	340.2	364.6	374.7	–2.5
2.5PLMTPU	325.6	366.0	376.1	–2.7
5PLMTPU	334.2	364.5	373.7	–2.5
7.5PLMTPU	330.4	365.6	377.3	–2.1
10PLMTPU	321.8	363.4	371.7	–1.9

stresses induce void nucleation and craze leading to the brittle failure mechanism of PLA. However, the incorporation of ATPU and MTPU flexible grafted polymer moieties resulted in the delocalization of the concentrated triaxial stresses of PLA and consequently the lowering of yield stress and broadening of yield peak. The blend samples exhibited a ductile mechanism of failure characterized by strain softening

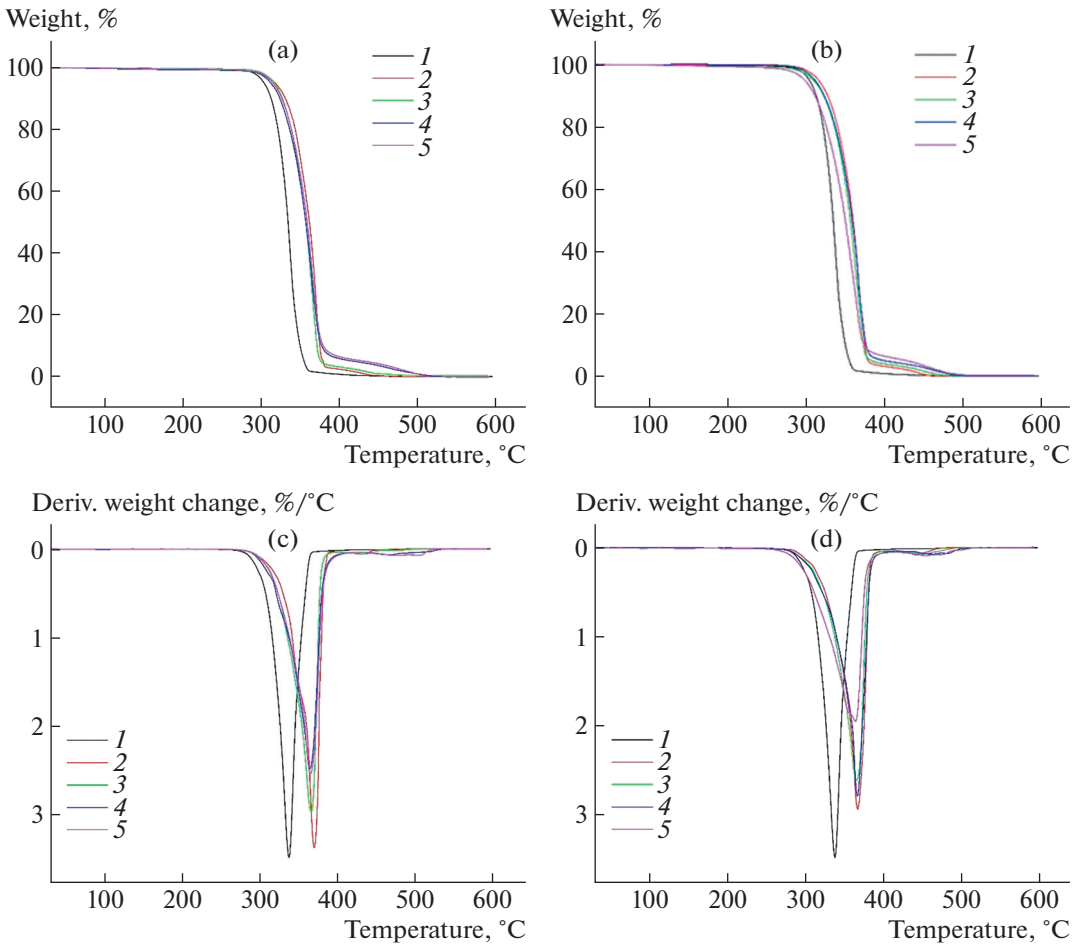

Fig. 3. (a, b) TGA and (c, d) DTG curves of (*1*) PLA, (a, c) (*2*) 2.5PLATPU, (*3*) 5PLATPU, (*4*) 7.5PLATPU, (*5*) 10PLATPU, (b, d) (*2*) 2.5PLMTPU, (*3*) 5PLMTPU, (*4*) 7.5PLMTPU, (*5*) 10PLMTPU.

followed by necking and strain broadening as suggested by the tensile characteristics of blends enlisted in Table 2.

The blends exhibited a primary increase in tensile strength and elongation at break compared to pure PLA and consequent decrease with increasing percent composition of compatibilized TPU. This may be attributed to the stress concentration effects of the TPU and the interactions of Acrylonitrile and Maleic anhydride on PLA.

The variation of relative tensile strength and normalized tensile strength with respect to the corresponding volume fractions of the respective blends revealed that all blends had relative tensile strength value in the range of unity, suggesting that the strain softening effect of the less hard TPU blend component did not drastically affect the strength property of the matrix material. It was further noted that all blends had normalized tensile strength values greater than unity, volume fraction $0.03\Phi_d$ being four folds for PLATPU and two folds for PLMTPU blends. This may be attributed to the softening effect of TPU being countered effectively by compatibilization and the consequent crystallinity values. Tensile strength of PLA/TPU blends was found to initially increase and then decrease in correlation to percent crystallinity values. This may be the result of a positive interference and the enhanced nucleation and PLA crystal growth supported by the presence of a flexible substituent in TPU, as evident from the DSC studies. However, the tensile strength values were greater than that of pure PLA, suggesting a positive interaction mechanism between the substituent groups and PLA as evident from Table 2.

Experimental values of tensile strengths of blends were compared to theoretical predictions of modelling, viz, rule of mixture (Eq. (3)):

$$\frac{\sigma_b}{\sigma_m} = \left[\frac{\sigma_b}{\sigma_m} - 1\right] \times \Phi_d + 1, \quad (3)$$

where σ is the tensile strength and subscripts b, m, and d signify the blend, continuous phase and discrete phase respectively.

Nicolais-Narki's model (NN Model) (Eq. (4)) is significant in that it defines the interface interaction constant k as a function of blend structure. For spherical inclusions, $k = 1.21$ represents the extreme case of poor adhesion and interface adhesion increases through values of $k < 1.21$ to $k = 0$, considered for sufficient adhesion so that no decrease in polymer matrix strength is witnessed [44].

$$\frac{\sigma_b}{\sigma_m} = 1 - k\Phi_d^{2/3}. \quad (4)$$

In employing porosity model, (Eq. (5)), for theoretical predictions, stress concentration is described by the stress concentration parameter α, such that a high value of α signifies a higher extent of stress concentrations and thereby a greater decrease in tensile strength is witnessed [44]. The model assumes dispersed phase as non-interacting pores or voids in the continuous phase.

$$\frac{\sigma_b}{\sigma_m} = e^{(-\alpha\Phi_d)}. \quad (5)$$

The non-interacting discrete phase, as per the assumptions of porosity model, acts as areas of stress concentration for lack of adhesion at phase boundaries. However, in the Béla Pukánszky model, (Eq. (6)), tensile strength of the blend is determined by tensile strength of the continuous phase, effective load-bearing cross-section and interaction between the two phases, B [45]. The parameter B signifies the load bearing capacity of the dispersed phase and is further dependent on the interface, contact area and properties, as in aggregation decreasing the physical interfacial contact area between the two polymeric blends, consequently decreasing the value of B.

$$\frac{\sigma_b}{\sigma_m} = \left[\frac{(1-\Phi_d)}{(1+2.5\Phi_d)}\right] \times e^{(B\Phi_d)}. \quad (6)$$

The variations of experimental and theoretical values tensile strength of the blends against Φ_d values are plotted in the Fig. 4, wherein, NN Model and Porosity model assumes discrete and continuous phases to be non-interacting for being non-adherent type and whereby the ultimate tensile strength is a function of either area fraction or volume fraction of the dispersed phase. The characteristic parameters of the models, k, α and B for NN Model, Porosity model and Béla Pukánszky model respectively, were calculated and are listed in Table 3. The negative average values of k were indicative of a good degree of adhesion between the constituents of both PLATPU and PLMTPU blends and subsequently denoted smaller extent of weakness in the blend structure [46]. Values of Porosity model α constant denotes further a lesser extent of stress concentration and positive values of B constant depicting the load bearing capacity of the constituents of the blends suggest negligible amount of aggregation and excellent interactions at polymer–polymer interface.

Tensile Modulus values of both PLATPU and PLMTPU blends were observed to decrease with decrease in percent crystallinity of the blends. The decreasing trend in moduli values was attributed to the dispersed phase acting as a flexibilizing agent facilitating nonspecific phase interaction with the continuous phase PLA. The relative modulus, E_b/E_m of the blends were plotted against Φ_d values (Fig. 5). The plots showed a decrease in relative moduli values with increasing Φ_d values, implying flexibility of the constituent TPU and decrease in crystallinity lead to significant softening of the continuous phase, PLA.

Variations of tensile modulus of the blends were further, compared with various theoretical prediction

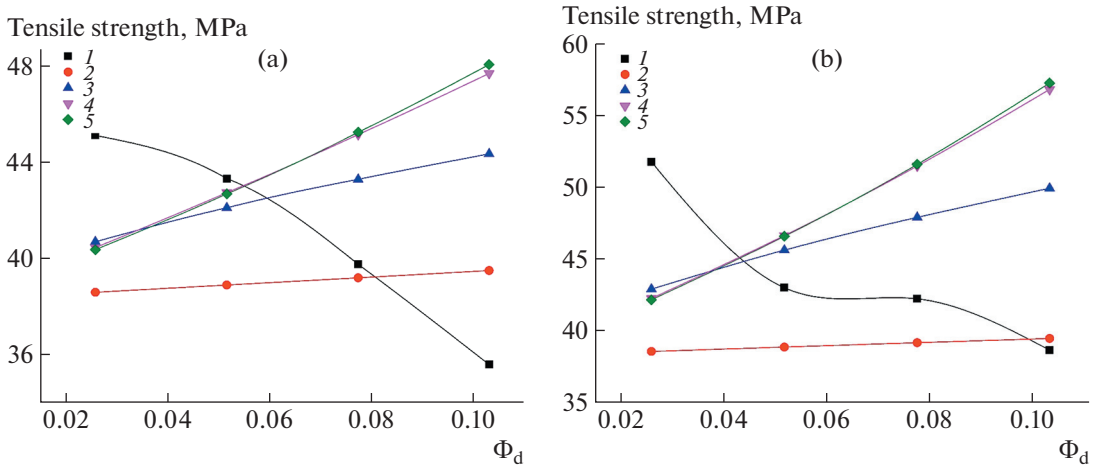

Fig. 4. Variation of (*1*) tensile strength, (*2*) rule of mixture, (*3*) NN model, (*4*) porosity model, (*5*) BP model with different volume fraction of blends (a) PLATPU and (b) PLMTPU.

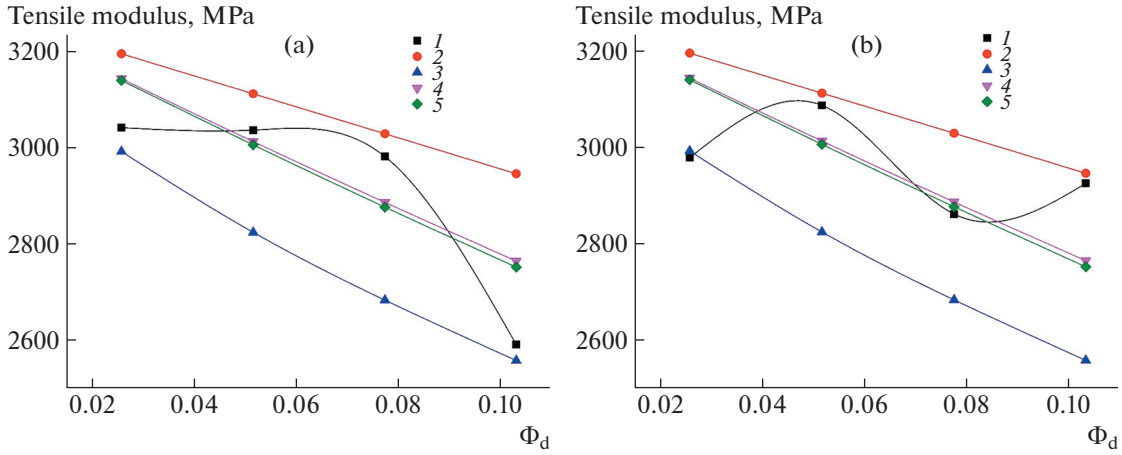

Fig. 5. Variation of (*1*) tensile modulus, (*2*) rule of mixture, (*3*) foam model, (*4*) KUT model-Adh, (*5*) KUT model-NonAdh with different volume fraction of blends (a) PLATPU and (b) PLMTPU.

models so as to evaluate the blend structure. Rule of mixture (Eq. (7)) considers perfect adhesion and perfect dispersion of the spherical inclusions, dispersed phase, in the continuous phase [47].

$$\frac{E_b}{E_m} = \left[\frac{E_d}{(E_m - 1)}\right] \times \Phi_d + 1, \quad (7)$$

where E_b and E_m are modulus value of blend system and PLA matrix respectively. E_d value corresponds to the modulus value of ATPU and MTPU.

On the other hand, Foam model (Eq. (8)), proposed by Cohen and Ishai, considers the dispersed phase as a non-interacting phase equivalent to a void or pore whereby, E_d/E_m is rendered negligible [44].

$$\frac{E_b}{E_m} = [1 - \Phi_d^{2/3}]. \quad (8)$$

The Kerner–Uernura–Takayanagi (KUT) model considers the blends as spherical inclusions of discrete phase in a continuous matrix with Poisson's ratio (ν_m) = 0.5 and with two boundary conditions of perfect adhesion at blend interface (Eq. (9)) and that of no-adhesion (Eq. (10)) [48].

$$\frac{E_b}{E_m} = \frac{(7 - 5\nu_m)E_m - (8 - 10\nu_m)E_d - (7 - 5\nu_m)(E_m - E_d)\Phi_d}{(7 - 5\nu_m)E_m + (8 - 10\nu_m)E_d + (8 - 10\nu_m)(E_m - E_d)\Phi_d}, \quad (9)$$

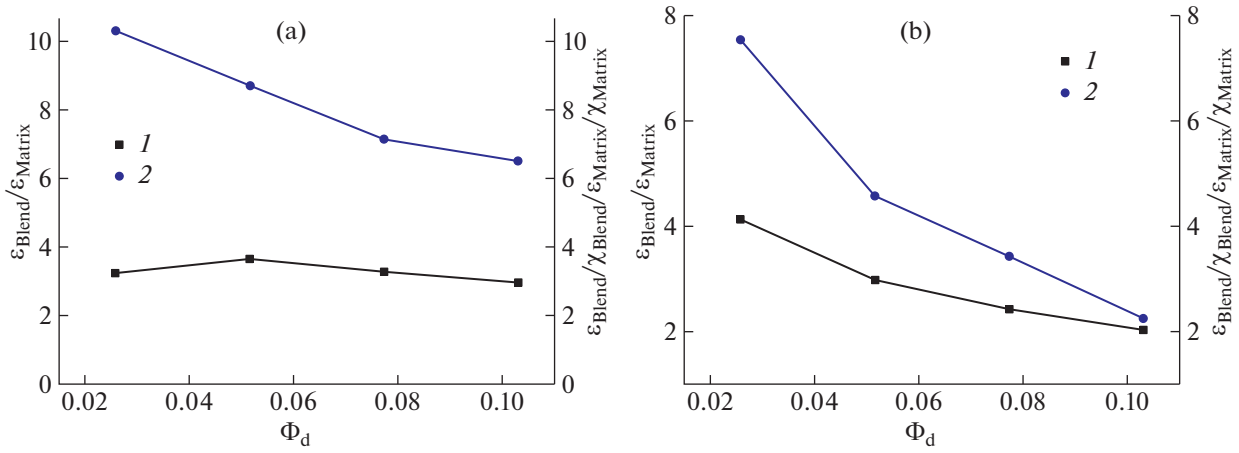

Fig. 6. Variation of (*1*) relative and (*2*) normalized elongation at break of blends (a) PLATPU and (b) PLMTPU.

$$\frac{E_b}{E_m} = \frac{(7-5\nu_m)E_m - (7-5\nu_m)E_m\Phi_d}{(7-5\nu_m)E_m + (8-10\nu_m)E_m\Phi_d}. \quad (10)$$

Figure 5 represents the variations of tensile modulus of blends to their prediction models. The initial tensile modulus values of $\Phi_d = 0.03$ for both PLATPU and PLMTPU follows the foam model, indicating that the dispersed phases, compatibilized TPU, were acting as a non-interacting phase with the continuous phase, PLA, viz. as a void or pore. However, for increasing Φ_d values, both blends are found to follow KUT model for perfect adhesion between the blend components closely reaching for the rule of mixture, indicating an improvement in interaction and compatibilization achieved. At $\Phi_d = 0.08$, the modulus values for PLATPU blend indicate the blend components again following the foam model and thereby indicating a corresponding decline in the magnitude of positive interaction between the blend components whereas the moduli values of PLMTPU indicate an enhanced adhesion mechanism for the moduli values follow the rule mixture closely.

The variance of elongation at break for PLATPU and PLMTPU blends were shown in Table 2. The elongation at break values for both PLATPU and PLMTPU blends were found to be improved in comparison to virgin PLA, as shown in Fig. 6. This is attributed to the increased PLA amorphization and flexibility introduced by the compatibilized TPU moieties.

In the context of PLATPU, the values showed an initial increase till $\Phi_d = 0.05$ and then decrease, suggesting the reason for improvement of elongation values from that of the matrix to be matrix softening, as indicated by the decrease in corresponding moduli values, whereas the variance in elongation with respect to Φ_d values was attributed to the effect of matrix softening and improved flexibility of the blend.The results suggest a positive interaction between the grafted Acrylonitrile group of TPU with PLA matrix and leads to a decrease in normalized elongation at break. The effect of matrix softening and flexibility introduced by the discrete phase (compatibilized TPU) analyzed with the normalized elongation at break. Similarly, in the case of PLMTPU, the decreased elongation with increasing Φ_d values may be the result of positive interactions of the maleated TPU and PLA matrix. The results revealed a less effective matrix softening and flexibility by MTPU.

Impact strength of PLATPU and PLMTPU blends and their percent increase are presented in Table 2. The variance of relative notched impact strength of PLATPU and PLMTPU blends and normalized impact strength denoting the enhancement of relative impact strength sans the effect of PLA matrix crystallinity, are shown in Fig. 7.

The relative notched impact strength values of both PLATPU and PLMTPU blends are found to be higher than that of the virgin matrix PLA. However, the increasing trend on relative impact strength were observed up to Φ_d value of 0.08 and then decrease for Φ_d of 0.10. This may be due to the combined effects of matrix softening and flexibility imparted by the discrete phase and positive interactions between the compatibilized moieties viz. Acrylonitrile grafts and maleate groups on TPU, with PLA matrix.

Similarly, the normalized impact strength values showed no significant variation to a near linear trend with the first significant decrease witnessed only for Φ_d of 0.10. This may be due to the enhanced ductility of the blend. Even though under impact condition, the

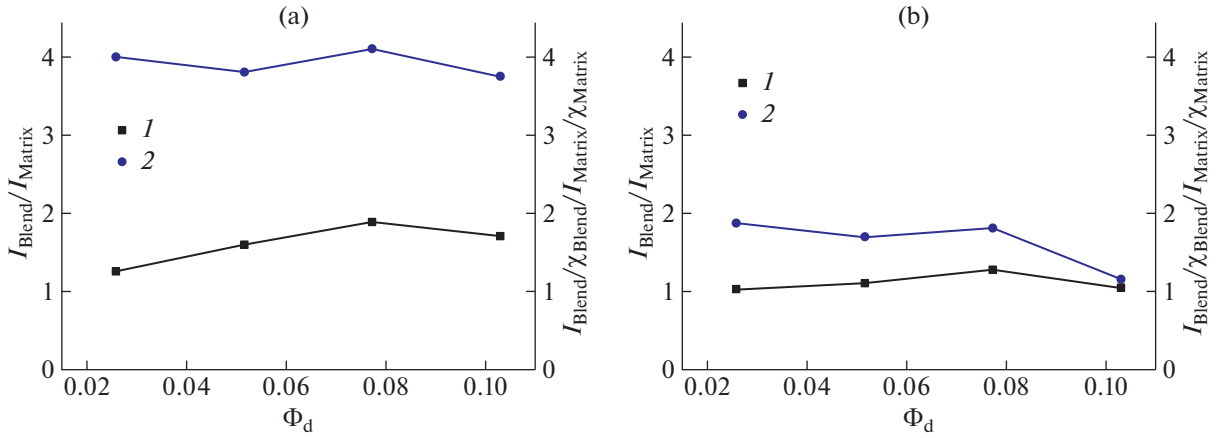

Fig. 7. Variation of (*1*) relative and (*2*) normalized impact strength of blends (a) PLATPU and (b) PLMTPU.

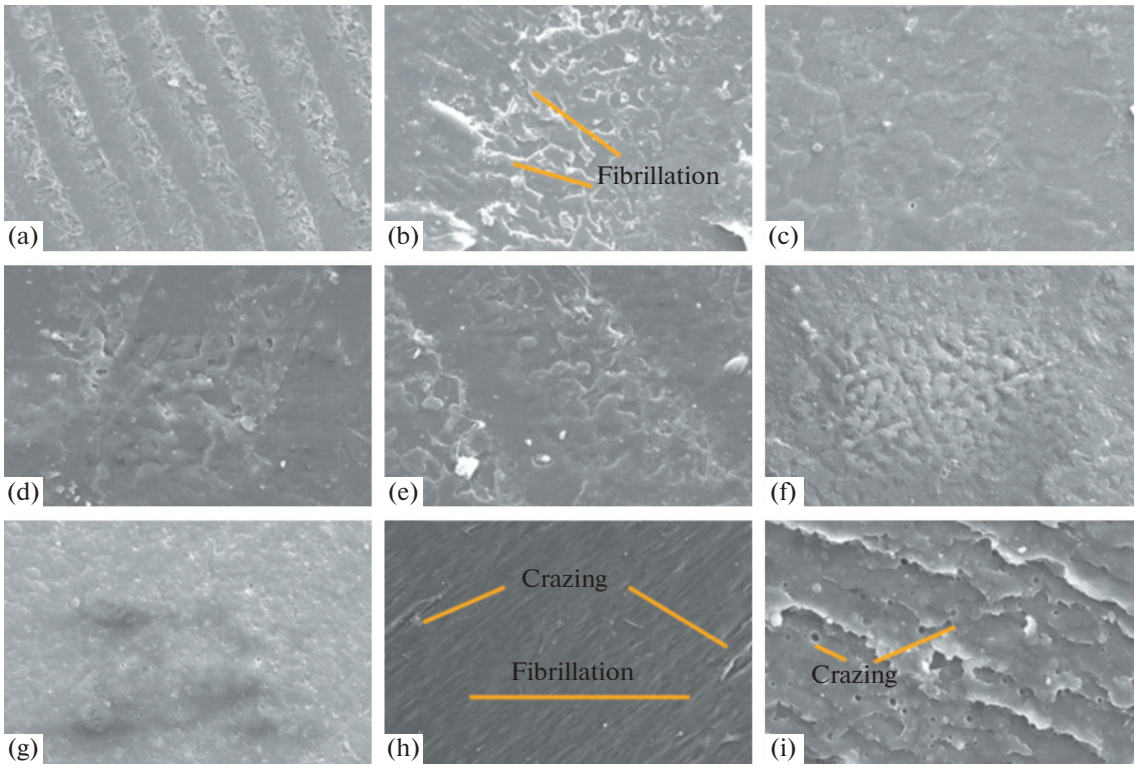

Fig. 8. SEM images of (a) PLA, (b) 2.5PLATPU, (c) 5PLATPU, (d) 7.5PLATPU, and (e) 10PLATPU; (f) 2.5PLATPU, (g) 5PLATPU, (h) 7.5PLATPU, and (i) 10PLATPU with magnification 100×.

percent crystallinity of the blend increases, the flexibility introduced by the TPU moieties increased the extent of shear yielding and also improved the cavitation owing to the high compatibilization effect.

The impact fractured microstructures of PLA, PLATPU, and PLMTPU blends were investigated by SEM. As shown in Fig. 8, PLA exhibits typical brittle fracture surfaces. Whereas, obvious toughening mechanism initiated by crazing, fibrillation, and shear yielding can be seen in the PLATPU and PLMTPU blends and it can be connected to its high impact strength. Whitened regions in the blends can be connected with the partial miscibility of the blend components and it can be due to the yielding of TPU phase at the interface region which dissipates energy indicating plastic deformation of PLA matrix with shear yielding [49]. It was also evident from the micrographs that different degrees of interfacial debonding led to the formation of voids, deforming the surrounding matrix (i.e. crazing). Crazing and fibrillation are more evi-

dent in the blend system especially on the PLATPU blends [50]. Impact energy was dissipated by crazing wherein the fibrils absorbed energy until they ruptured and this leads to improvement in the impact toughness of the blends [48]. The cross-section images showed more uniform distribution of two phases that may prove the high compatibilization. This is an effect of flexibilization of PLA imparted by TPU component, and the effective stress transfer mechanism brought forward by the compatibilization effect.

CONCLUSIONS

In this study, we reported for the first time blending of PLA with acrylonitrile and maleic anhydride grafted TPU. The PLA was successfully toughened with very low volume fractions of ATPU and MTPU via reactive melt blending technique. The modified TPU acted as a flexibilizing agent and the grafted moieties effected positive interactions with PLA, resulting in improved mechanical properties without adversely affecting any inherent properties. The PLATPU blends exhibited a maximum increase of 89% in impact strength for $\Phi_d = 0.08$ composition, 266% increase in elongation at break for $\Phi_d = 0.05$ and 18% increase in tensile strength for $\Phi_d = 0.03$, whereas, PLMTPU blends exhibited maximum increase of 28% in impact strength for $\Phi_d = 0.08$, 311% increase in elongation at break and 35% increase in tensile strength for $\Phi_d = 0.03$ compositions. Meanwhile it was noted that the decrease in tensile modulus was in tolerable limits in comparison to virgin PLA. Further the mechanical performance of blends was compared with various theoretical models, so as to evaluate the extent of the effected compatibilization between PLA and TPU. The compatibilization of the blends was also obvious with the decrease in the T_g, and improvement in the thermal stability. The interactions between the grafted moieties and PLA were also confirmed by the degree of crystallinity of the blends. The observations were further substantiated by morphology analysis. The proposed blend system of PLA is proven by its higher mechanical properties, thermal stability and flexibility and this allow its use in many fields especially as a potential aspirant in 3D printing.

CONFLICT OF INTEREST

The authors declare that they have no conflict of interest.

REFERENCES

1. A. Lasprilla, G. Martinez, B. N. H. Lunelli, A. L. Jardini, and R. M. Filho, Biotechnol. Adv. **30**, 321 (2012).
2. M. Bijarimi, S. Ahmad, and A. M. Alam, Polym. Bull. **74** (8), 3301 (2017).
3. K. Coskun, A. Mutlu, M. Dogan, and E. Bozacı, J. Thermoplast. Compos. Mater. **34** (8), 1066 (2021).
4. M. Allahdady, S. Hedjazi, M. Jonoobi, A. Abdulkhani, and L. Jamalirad, Nord. Pulp Pap. Res. J. **34** (3), 239 (2019).
5. K. Oksman, M. Skrifvars, and J.-F. Selin, Compos. Sci. Technol. **63**(9), 1317 (2003).
6. A. Pappu, K. L. Pickering, and V. K. Thakur, Ind. Crops Prod. **137**, 260 (2019).
7. B. Asaithambi, G. Ganesan, and S. A. Kumar, Fibers Polym. **15**, 847 (2014).
8. H. Kyutoku, N. Maeda, H. Sakamoto, H. Nishimura, and K. Yamada, Carbohydr. Polym. **203**, 95 (2019).
9. D. Vrsaljko, D. Macut, and V. Kovačević, J. Appl. Polym. Sci. **132** (6), 41414 (2015).
10. T.-W. Lee and Y. G. Jeong, Compos. Sci. Technol. **103**, 78 (2014).
11. A. K. Mohapatra, S. Mohanty, and S. Nayak, Polym. Compos. **35**, 283 (2014).
12. K. Pongtanayut, C. Thongpin, and O. Santawitee, Energy Procedia **34**, 888 (2013).
13. N. Ljungberg, D. Colombini, and B. Wesslén, J. Appl. Polym. Sci. **96** (4), 992 (2005).
14. F. Jing and M. A. Hillmyer, J. Am. Chem. Soc. **130** (42), 13826 (2008).
15. L. Labrecque, R. Kumar, V. Dave, R. Gross, and S. McCarthy, J. Appl. Polym. Sci. **66** (8), 1507 (1997).
16. B. H. Li and M. C. Yang, Polym. Adv. Technol. **17** (6), 439 (2006).
17. M. L. Robertson, K. Chang, W. M. Gramlich, and M. A. Hillmyer, Macromolecules **43** (4), 1807 (2010).
18. H. Li and M. A. Huneault, Polymer **48** (23), 6855 (2007).
19. X. Zhao, H. Hu, X. Wang, X. Yu, W. Zhou, and S. Peng, RSC Adv. **10** (22), 13316 (2020).
20. X. Zheng, C. Zhang, C. Luo, G. Tian, L. Wang, and Y. Li, Ind. Eng. Chem. Res. **55** (11), 2983 (2016).
21. S. K. Dogan, E. A. Reyes, S. Rastogi, and G. Ozkoc, J. Appl. Polym. Sci. **131** (10), 40251 (2014).
22. H. Hong, J. Wei, Y. Yuan, F. P. Chen, J. Wang, X. Qu, and C. S. Liu, J. Appl. Polym. Sci. **121** (2), 855 (2011).
23. F. Feng and L. Ye, J. Appl. Polym. Sci. **119** (5), 2778 (2011).
24. H. Hong, J. Wei, Y. Yuan, F. P. Chen, J. Wang, X. Qu, and C. S. Liu, J. Appl. Polym. Sci. **121** (2), 855 (2011).
25. Y. Kahraman, B. Özdemir, V. Kılıç, Y. A. Goksu, and M. Nofar, J. Appl. Polym. Sci. **138** (20), 50457 (2021).
26. N. T. Kilic, B. N. Can, M. Kodal, and G. Özkoç, Prog. Rubber, Plast. Recycl. Technol. **37** (4), 301 (2021).
27. X. Su, S. Jia, L. Cao, and D. Yu, J. Appl. Polym. Sci. **138** (3), 51014 (2021).
28. S. M. Kang, M. S. Kang, S. H. Kwon, H. Park, and B. K. Kim, J. Polym. Eng. **34** (6), 555 (2014).
29. T. Sehgal and S. Rattan, Int. J. Polym. Sci. **2010**, 147581 (2010).
30. E. Baştürk, S. Madakbaş, and M. V. Kahraman, Mater. Res. **19**, 434 (2016).
31. L. Xing, L. Liu, X. Wang, and Y. Huang, "Preparation of Aramid/bn Reinforced Self-Healable Nanocomposites and Their Performance," in *Proceedings of 21st International Conference on Composite Materials, Xi'an, China, 2017* (Xi'an, 2017).

32. A. De León, A. Domínguez-Calvo, and S. Molina, Mater. Des. **182**, 108044 (2019).
33. J. Lisperguer, C. Nunez, and P. Perez-Guerrero, J. Chil. Chem. Soc. **58** (4), 1937 (2013).
34. D. Stewart, Ind. Crops Prod. **27**(2), 202 (2008).
35. E. Ruiz-Silva, M. Rodríguez-Ortega, L. C. Rosales-Rivera, F. J. Moscoso-Sánchez, D. Rodrigue, and R. González-Núñez, Polymers **13** (2), 217 (2021).
36. Y. S. Lee and K. Ha, J. Elastomers Plast. **53** (5), 402 (2021).
37. Y. S. Lee and K. R. Ha, World J. Text. Eng. Technol. **5**, 77 (2019).
38. L. C. Arruda, M. Magaton, R. E. S. Bretas, and M. M. Ueki, Polym. Test. **43**, 27 (2015).
39. A. U. Birnin-Yauri, N. A. Ibrahim, N. Zainuddin, K. Abdan, Y. Y. Then, and B. W. Chieng, Polymers **9** (5), 165 (2017).
40. Y. Zhou, L. Luo, W. Liu, G. Zeng, and Y. Chen, Adv. Mater. Sci. Eng. **2015**, 393582 (2015).
41. N. T. Kilic, B. N. Can, M. Kodal, and G. Ozkoc, AIP Conf. Proc. **1914**, 070005 (2017).
42. Y. G. Devrim, Z. M. Rzaev, and E. Pişkin, Polym. Bull. **59** (4), 447 (2007).
43. N. F. Alias and H. Ismail, Polym.-Plast. Technol. Mater. **58** (13), 1399 (2019).
44. N. Tomar and S. Maiti, J. Appl. Polym. Sci. **104** (3), 1807 (2007).
45. A. Kiss, E. Fekete, and B. Pukánszky, Compos. Sci. Technol. **67** (7-8), 1574 (2007).
46. V. L. Finkenstadt, C.-K. Liu, R. Evangelista, L. Liu, S. C. Cermak, M. Hojilla-Evangelista, and J. Willett, Ind. Crops Prod. **26** (1), 36 (2007).
47. J. H. Mina, A. V. González, and M. F. Muñoz-Vélez, Polymers **12** (1), 58 (2020).
48. M. Broz, D. L. VanderHart, and N. Washburn, Biomaterials **24** (43), 4181 (2003).
49. K. A. Afrifah and L. M. Matuana, Macromol. Mater. Eng. **295** (10), 802 (2010).
50. F. Yu and H.-X. Huang, Polym. Test. **45**, 107 (2015).